INVESTIGATIONS ON THE EXPERIMENTALLY PRODUCED CHONDRULES: CHEMICAL COMPOSITIONS OF OLIVINE AND GLASS AND FORMATION OF RADIAL PYROXENE CHONDRULES

Akira TSUCHIYAMA, Hiroko NAGAHARA and Ikuo KUSHIRO

Geological Institute, Faculty of Science, University of Tokyo, 3-1, Hongo 7-chome, Bunkyo-ku, Tokyo 113

Abstract: Recently, textures of chondrules have been reproduced experimentally by cooling liquids of chondrule compositions, and thereby the cooling rate of chondrules during their crystallization has been estimated (TSUCHIYAMA *et al.*: Earth Planet. Sci. Lett., **48**, 155, 1980). In the present study, the chemical compositions of olivine and glass of run products in the previous experiments were determined. Olivine crystals are normally zoned. The chemical compositions of glasses are extremely enriched in SiO_2 due presumably to disequilibrium crystallization of olivine by rapid cooling. Similar glasses have been observed in unequilibrated chondrites.

Additional experiments were also performed to produce radial pyroxene texture which could not be produced in the previous experiments. The radial pyroxene was formed by reaction between radial olivine and residual SiO_2-rich liquid without changing its texture. This process might be a possible mechanism of formation of radial pyroxene texture of chondrules.

1. Introduction

TSUCHIYAMA *et al.* (1980) reproduced textures of chondrites in their experiments by cooling melts of three different chondrule compositions (H chondrite). They concluded that the bulk composition is the main factor to control the textural variations of chondrules, while the cooling rate is subordinate to the compositional effect. They estimated the cooling rate of chondrules when crystallization occurred (*i.e.*, 50–120 deg/min) by comparing the textures of natural chondrules with those of experimental ones.

In the present study, the chemical compositions of the run products of the previous experiments were determined by electron microprobe analysis to compare the chemical compositions of natural chondrules with those of the run products. Also additional experiments have been conducted to produce radial pyroxene texture which could not be produced in the previous experiments.

2. Experimental Technique

Quantitative point analyses of the run products were performed with a HITACHI X560S electron-probe microanalyzer (FUJIMAKI and AOKI, in preparation) and scanning analyses were performed with a JEOL 5 type electron-probe microanalyzer.

The method and the starting materials of the experiments to produce radial pyroxene were the same as those of the previous experiments (TSUCHIYAMA *et al.*, 1980). Phase determination of the run products was performed by X-ray powder diffraction method and with an electron-probe microanalyzer.

3. Results

3.1. Textures and chemical compositions

All the charges obtained in the previous experiments have residual glass and olivine as crystalline phase. The chemical compositions of the starting materials (Sample Nos. 1, 2 and 3) are given in Table 1.

Table 1. Chemical compositions and CIPW norms of the starting materials.

Sample No.	1	2	3	Sample No.	1	2	3
SiO_2	44.93	46.10	55.21	Or	0.17	0.67	0.45
Al_2O_3	4.61	3.21	4.71	Ab	11.32	8.70	19.45
TiO_2	0.02	0.10	0.00	An	4.67	1.14	2.31
FeO	15.04	15.37	11.79	C	0.66	0.98	-
MnO	0.08	0.39	0.15	Di Wo	-	-	0.24
MgO	33.23	30.63	22.21	Di En	-	-	0.16
CaO	0.96	0.84	0.60	Di Fs	-	-	0.07
Na_2O	1.34	1.03	2.53	Hy En	10.50	25.91	48.62
K_2O	0.03	0.11	0.08	Hy Fs	3.52	9.62	19.06
Cr_2O_3	0.04	0.60	0.28	Ol Fo	50.62	35.29	4.56
NiO	0.06	0.02	0.00	Ol Fa	18.74	4.43	1.98
P_2O_5	0.01	0.25	0.01	Cm	0.07	0.87	0.40
				Il	0.05	0.20	0.00
				Ap	0.03	0.61	0.03
Total	100.35	98.65	97.37	Total	100.35	98.40	97.33

Scanning analyses revealed that olivine crystals are normally zoned (Fo_{94} to Fo_{83} for Sample No. 1, Fo_{92} to Fo_{77} for Sample No. 2 and Fo_{89} to Fo_{78} for Sample No. 3) and that the residual glass has compositional gradients towards the olivine crystals. Examples are given in Fig. 1.

The chemical compositions of olivine and residual glass are given in Tables 2

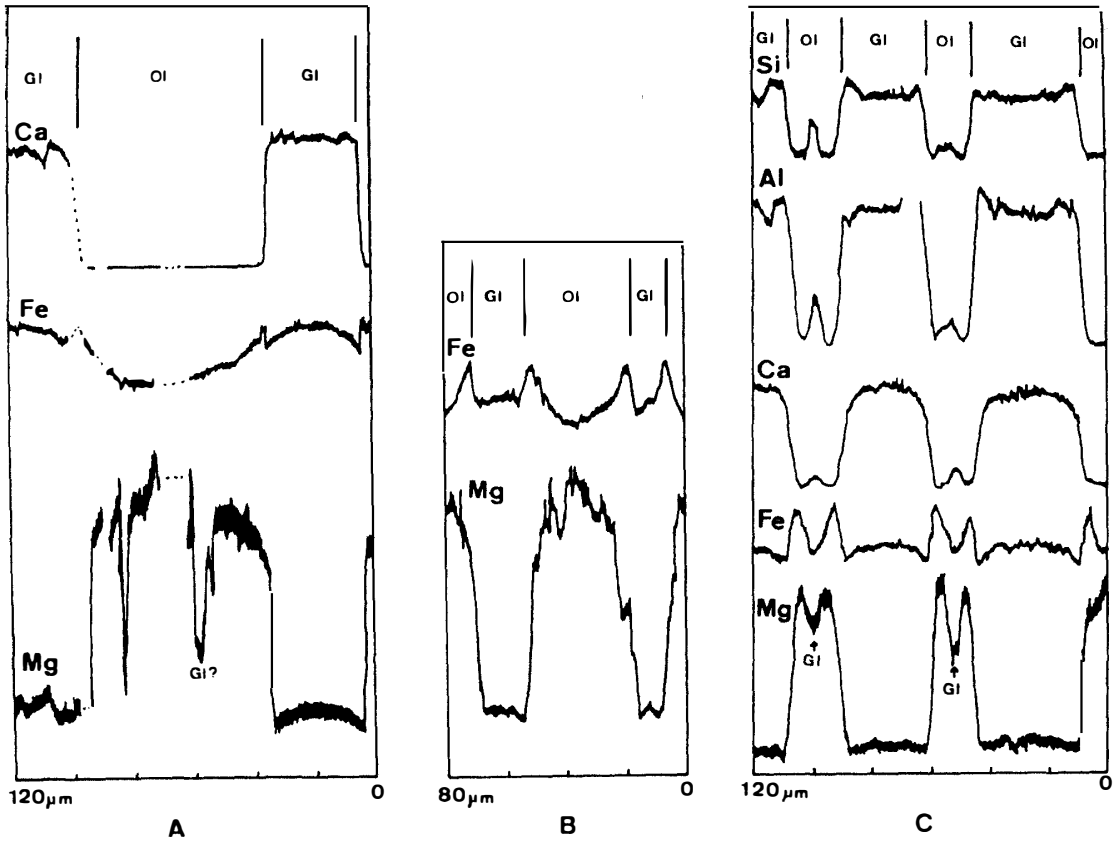

Fig. 1. Scanning patterns of run products in the previous experiments. (A) Porphyritic texture on Sample No. 1 at cooling rate 50 deg/min; (B) barred-olivine texture on Sample No. 2 at cooling rate 67 deg/min; (C) radial texture on Sample No. 3 at cooling rate 20 deg/min (Glass films are present in olivine crystals). Note that glass (Gl) has compositional gradients for each element except for Ca.

and 3. As shown in Table 2, Na is significantly low in the charges with slow cooling rates (less than 50 deg/min) probably due to Na vaporization. They are also plotted onto the SiO_2-MgO-FeO system based on MUAN and OSBORN (1965) (Fig. 2). The compositions of the residual glass are rich in SiO_2 and are plotted beyond the reaction line between olivine and protoenstatite fields. No systematic variations in compositions of olivine and glass are observed. Scatter of the FeO/MgO ratio of the residual glass is partly due to the iron loss to the Pt-wire. Fe-Mg distribution coefficient between olivine rim and glass in contact with it, $K_D=(FeO/MgO)^{ol}/(FeO/MgO)^{liq}$, ranges from 0.12 to 0.28, which is smaller than the equilibrium value (about 0.30) by ROEDER and EMSLIE (1970). This is probably due to the chemical inhomogeniety of olivine, especially the steep zoning near the rim of olivine as shown in Fig. 1.

Table 2. Chemical compositions of olivine obtained in the present study.

	Sample No. 1					Sample No. 2						Sample No. 3	
Cooling rate (°C/min) wt %	25B-3 133 core	23B-1 100-45 core	26B-1 50 rim	25C-3 20 rim	25C-6 20 core	9B-1 120 core	16-2 100 rim	16-5 100 core	15A-2 67	12-10 50 rim	4-1 36 core	21-2 20 ol+gl?	21-3 20 ol+gl?
SiO_2	40.61	40.85	40.22	40.15	41.29	40.94	39.54	40.29	40.36	40.27	41.06	40.95	40.75
Cr_2O_3	0.00	0.00	0.00	0.00	0.00	0.40	0.63	0.40	0.50	0.49	0.44	n.d.	0.26
FeO	10.42	9.48	11.03	13.74	7.59	7.42	15.19	10.58	11.77	11.75	8.05	10.88	11.68
MnO	0.00	0.05	0.12	0.00	0.07	0.26	0.83	0.23	0.35	0.33	0.24	0.17	0.13
MgO	48.57	49.56	47.69	46.47	51.03	50.49	43.83	48.31	47.27	47.00	50.12	47.58	46.86
NiO	n.d.	n.d.	n.d.	n.d.	n.d.	0.16	n.d.	n.d.	n.d.	n.d.	n.d.	0.13	0.12
CaO	0.07	0.01	0.10	0.09	0.08	0.00	0.12	0.09	0.00	0.11	0.06	0.06	0.08
Total	99.97	99.95	99.16	100.45	100.07	99.67	99.70	99.90	100.26	99.96	99.97	99.77	99.88
Si	0.999	0.999	1.000	0.997	1.000	0.998	0.999	0.993	0.997	0.998	0.999	1.010	1.008
Cr	0.000	0.000	0.000	0.000	0.000	0.008	0.013	0.008	0.005	0.010	0.008	–	0.005
Fe	0.220	0.194	0.229	0.285	0.154	0.151	0.321	0.218	0.243	0.244	0.164	0.224	0.242
Mn	0.000	0.001	0.003	0.000	0.001	0.005	0.008	0.005	0.007	0.007	0.005	0.004	0.003
Mg	1.780	1.807	1.766	1.719	1.824	1.834	1.651	1.776	1.741	1.737	1.818	1.749	1.728
Ni	–	–	–	–	–	0.003	–	–	–	–	–	0.003	0.002
Ca	0.002	0.000	0.003	0.002	0.002	0.000	0.003	0.002	0.000	0.003	0.002	0.002	0.002
Total	3.001	3.001	3.000	3.003	3.000	3.000	2.996	3.002	2.993	2.998	2.996	2.990	2.990
mol % Fo	89.0	90.3	88.5	85.8	92.3	92.4	83.7	89.1	87.7	87.7	91.7	88.6	87.7

n.d.: Not determined.

Table 3. Chemical compositions and CIPW norms of residual glass obtained in the present study.

	Sample No. 1				Sample No. 2				Sample No. 3	
Cooling rate (°C/min)	25B-3 133	26B-11 50	25C-4 20	25C-9 20	16-3 100	16-4 100	12-9 50	4-3 36	18A-1 133	21-4 20
wt %	rim	rim	rim	core	rim	core	rim	rim		rim
SiO_2	53.00	57.60	60.16	55.05	57.69	55.07	60.55	61.21	63.88	69.08
TiO_2	0.02	0.01	0.00	0.04	0.22	0.21	0.23	0.19	0.03	0.01
Al_2O_3	10.30	10.63	12.34	9.79	6.20	5.31	6.45	6.18	7.07	8.08
Cr_2O_3	0.09	0.06	0.11	0.12	0.89	1.05	0.99	0.88	0.32	0.26
FeO	18.27	12.74	12.81	16.38	16.71	19.05	15.45	12.28	11.43	9.07
MnO	0.14	0.12	0.12	0.14	0.47	0.65	0.53	0.47	0.21	0.13
MgO	12.00	13.45	8.26	13.29	10.75	12.26	9.10	12.04	10.32	6.41
CaO	4.20	4.60	5.14	4.57	4.84	5.20	5.80	5.15	3.81	3.97
Na_2O	1.41	0.66	0.79	0.33	1.72	1.48	0.52	0.56	2.71	1.97
K_2O	0.12	0.14	0.20	0.14	0.16	0.12	0.16	0.17	0.13	0.15
Total	99.54	100.02	99.93	99.84	99.65	100.39	99.87	99.13	99.91	99.86
Q	2.09	12.59	20.67	9.22	9.79	4.23	20.76	19.84	17.00	32.81
C	0.21	1.03	1.48	0.78	–	–	–	–	–	–
Or	0.70	0.82	1.18	0.82	0.94	0.70	0.94	1.00	0.76	0.88
Ab	11.92	5.58	6.68	2.79	14.54	12.51	4.39	4.73	22.92	16.66
An	20.83	22.81	25.49	22.66	8.72	7.49	14.79	13.84	6.74	12.76
Di Wo	–	–	–	–	6.37	7.64	5.83	4.88	5.07	2.89
Di En	–	–	–	–	2.92	3.48	2.55	2.61	2.68	1.38
Di Fs	–	–	–	–	3.40	4.09	3.26	2.11	2.23	1.46
Hy En	29.87	33.48	20.56	33.08	23.84	27.03	20.09	27.36	23.00	14.57
Hy Fs	33.77	23.59	23.74	30.26	27.78	31.74	25.70	22.09	19.09	15.41
Il	0.03	0.01	0.00	0.07	0.41	0.39	0.43	0.36	0.05	0.01
Total	99.46	99.95	99.82	99.73	98.76	99.35	98.79	98.85	99.59	98.87

Table 4. Conditions and results of the present experiments.

RUN	Sample No.	Cooling method #	Melting Temp. (°C)	Melting Dur. (min)	Cooling rate (°C/min)	Quench Temp. (°C)	Quench Dur. (hr)	Phase	Texture
103	3	1	1525	2	0.4	930	–	px, gl	radial
102	3	2	1525	2	100-4	800	–	ol, gl	radial
101	3	2	1525	2	100-20	1100	1.0	ol, gl	radial
104	3	2	1525	2	100-20	1100	36.5	ol, px, gl	radial

Cooling method: 1. Decreasing electric power was supplied to the furnace depending on the desired cooling rates. 2. Shutting off the electric power to the furnace, which produce non-linear cooling rate.

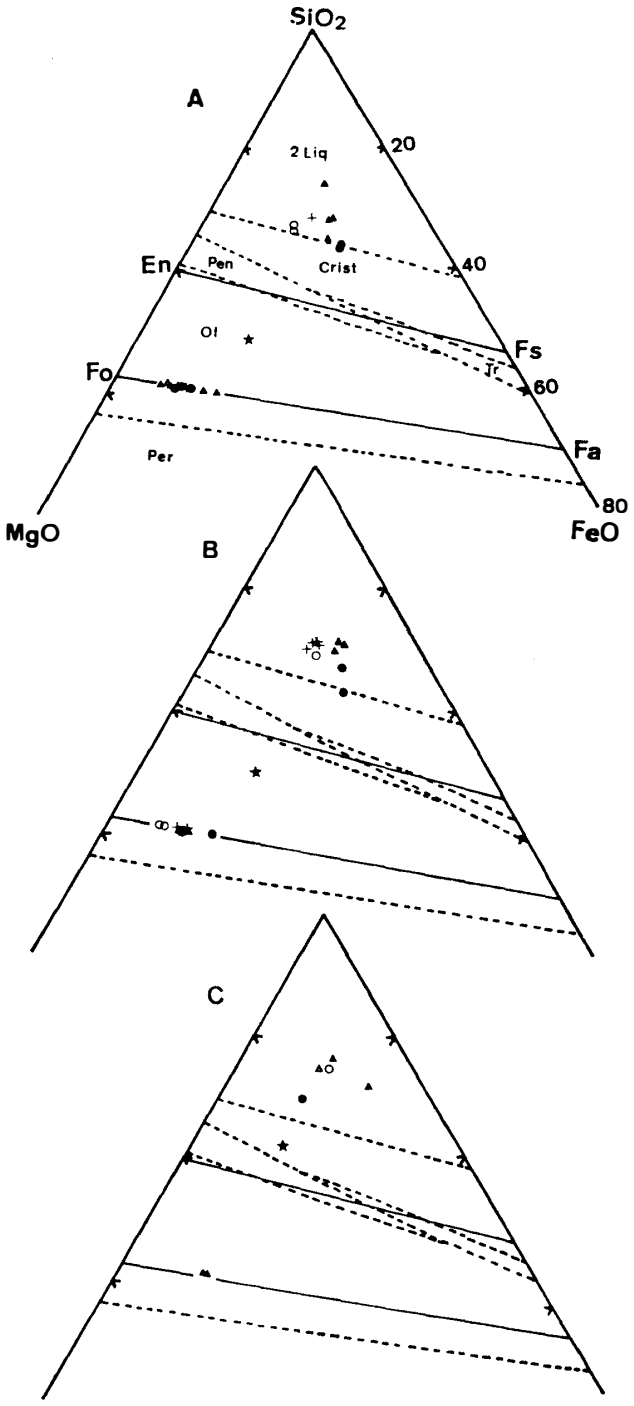

Fig. 2. Chemical compositions of olivine and residual glass plotted onto the SiO_2-MgO-FeO system based on MUAN *and* OSBORN *(1965). (A) Porphyritic texture on Sample No. 1. (cooling rates; open circle 400 deg/min, solid circle 133 deg/min, open triangle 100–45 deg/min (electric power shut off), cross 50 deg/min, solid triangle 20 deg/min); (B) bar-red-olivine texture on Sample No. 2. (cooling rates; open cicle 120 deg/min, solid circle 100 deg-/min, open triangle 67 deg/min, solid triangle 50 deg/min, cross 36 deg/min); (C) radial texture on Sample No. 3. (cooling rates: open circle 133 deg/min, solid circle 100 deg/min, open triangle 67 deg/min, solid triangle 20 deg/ min). In each figure, the compositions of the starting materials are shown by asterisks.*

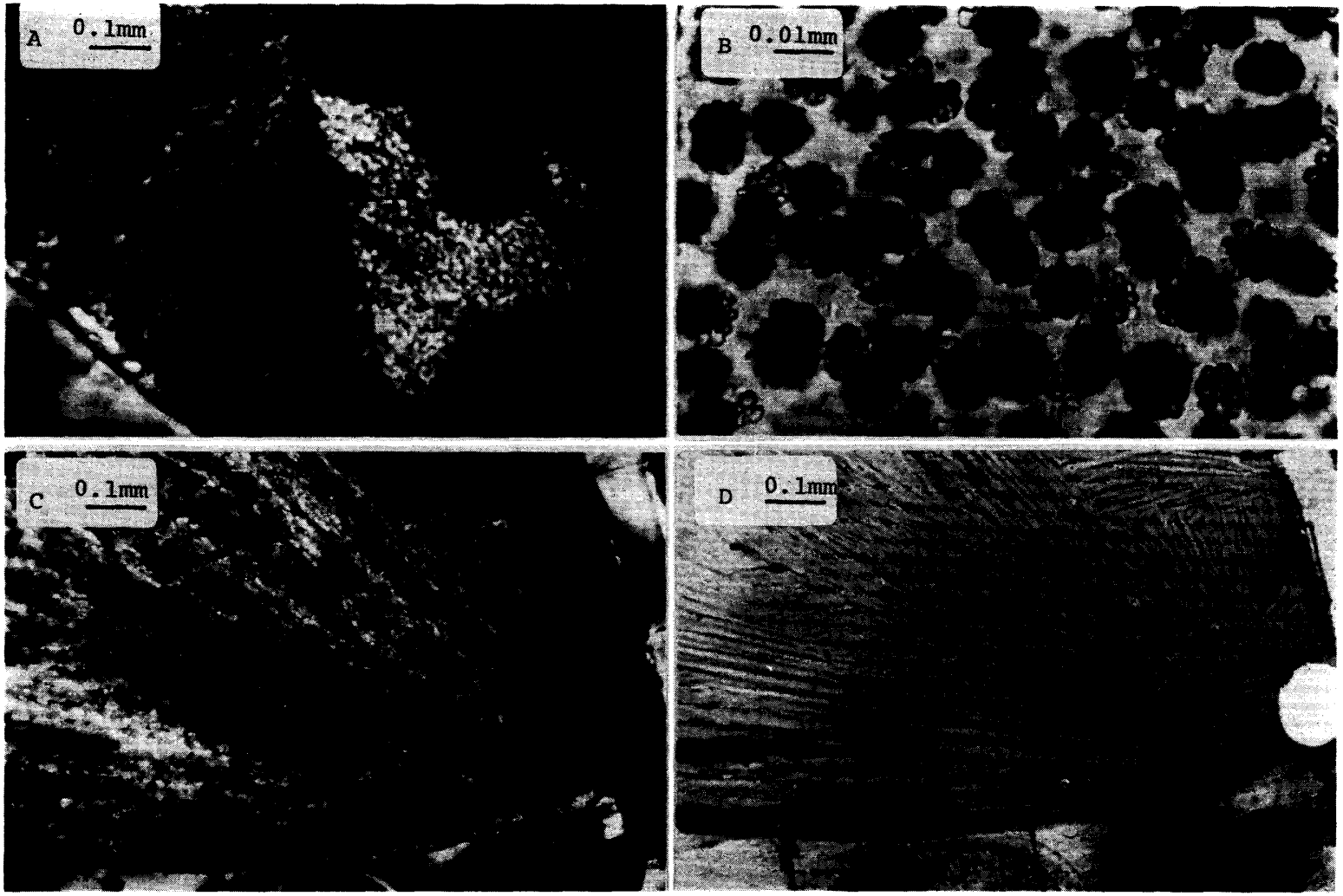

Fig. 3. Photomicrographs of thin sections of the run products obtained by the present experiments on Sample No. 3. (A) Radial texture of pyroxene (RUN 103, crossed nichols); (B) Radial texture of pyroxene (aggregates of fine droplets are glass and matrix is Ca-poor pyroxene); (C) Radial texture of olivine and pyroxene mixture (RUN 104, crossed nichols); (D) Radial texture of olivine and pyroxene mixture (olivine and pyroxene (white) and glass (gray) with reflected light).

3.2. Radial pyroxene

In the previous experiments, radial olivine was formed instead of radial pyroxene for Sample No. 3. Radial pyroxene is usually observed in natural chondrules with bulk compositions similar to that of Sample No. 3. Possible explanations for this discrepancy are as follows; (1) cooling rate of natural chondrules was much smaller than that of our experiments and (2) pyroxene was formed by reaction between early crystallized olivine and residual SiO_2-rich liquids.

Conditions and results of the additional experimental runs to produce radial pyroxene are given in Table 4. Radial pyroxene was produced in RUN 103 with a slow cooling rate (Fig. 3A); however, many fine droplets of residual glass were present in the radial pyroxene (Fig. 3B) which have never been found in natural radial pyroxene. In the other runs, radial olivine first crystallized at a higher temperature with the cooling rate of about 100 deg/min. Pyroxene appeared only in RUN 104 where the charge was kept at 1100°C for 36.5 hours after cooling (Figs. 3C and 3D, also see Fig. 6).

4. Discussion

4.1. Chemical compositions of olivine and glass

There are very little data of detailed chemical compositions of zoned olivine and glass in H3 chondrite. For this reason, the composition of olivine obtained in the experiments cannot be applied quantitatively to natural H3 chondrites. The zoning patterns of olivine (Fig. 1), however, are qualitatively similar to those in L3 chondrite (IKEDA and TAKEDA, 1979).

The compositional gradients in the residual glass (Fig. 1) have not been reported in unequilibrated chondrites. They should have been present in residual liquids of natural chondrules during their crystallization, but most of them were homogenized soon because diffusion in glass or liquid is very fast.

The chemical compositions of the residual glass are given in Fig. 2. The residual liquids are very silica-rich and they cannot be in equilibrium with olivine. Such a disequilibrium relation may be due to the rapid cooling and rapid crystallization of olivine. Similar relations have been found in unequilibrated chondrites which will be discussed later.

The chemical compositions of residual liquids in unequilibrated chondrites (VAN SCHMUS, 1967; IKEDA and TAKEDA, 1979; KIMURA and YAGI, 1980) are plotted onto the SiO_2-FeO+MgO-Al_2O_3 system (Fig. 4). where liquids associated only with olivine except for radial texture are plotted. The compositions of the glass obtained in the experiments are also plotted with olivine control lines. Wide variations of Al_2O_3 in natural glass may be mainly due to variations on initial Al_2O_3 contents in the chondrules and disequilibrium crystallization of olivine. CaO and Na_2O may

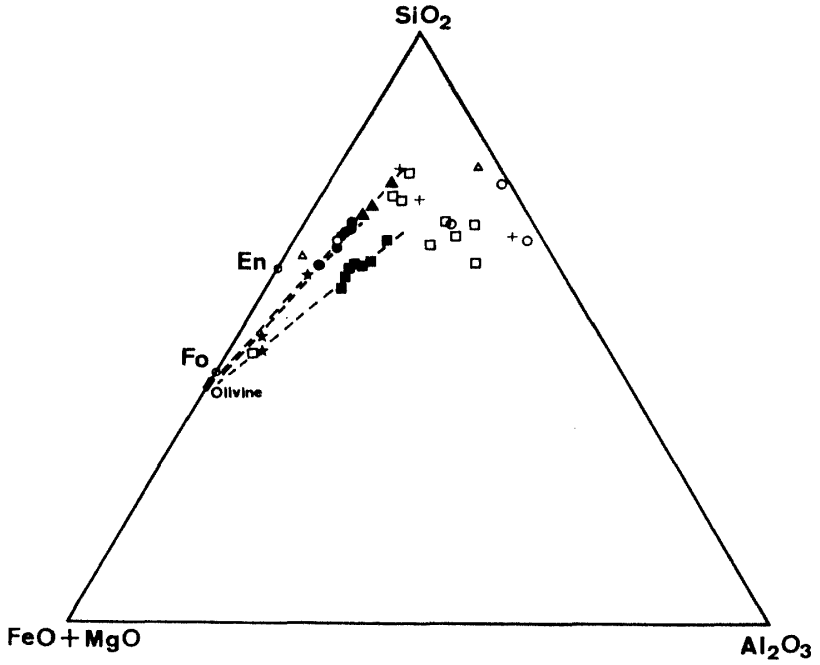

Fig. 4. Chemical compositions of residual glasses in L3 chondrites (open symbols) (VAN SCHMUS, 1967; IKEDA and TAKEDA, 1979; KIMURA and YAGI, 1980) and those obtained in the present study (solid symbols), plotted onto the SiO_2-FeO + MgO-Al_2O_3 system. Textures: square, porphyritic; circle, barred; triangle, radial. Glasses associated only with olivine are chosen except for open triangle. Cross shows compositions of residual glasses in H4 and H5 chondrites (KIMURA et al., 1979) texture of which is unknown. The compositions of the starting materials of the experiments are also shown by asterisks with olivine-control lines.

also be the case. Natural glass is usually rich in Na_2O (up to 16 wt%, VAN SCHMUS, 1967) although some of them are similar in Na_2O to those obtained in the rapidly cooled experiments (*e.g.* 100 deg/min or more).

Fig. 5 shows the compositions of the natural glass plotted onto the SiO_2-MgO-FeO system together with the experimental data, where Al_2O_3-rich glass is neglected. The FeO/MgO ratio of the natural glass is less than that of experimental one, although natural data are for L3 chondrites and iron was partly lost in the experiments. This is explained by assuming that crystallization of chondrules took place in an open system especially as to iron (IKEDA and TAKEDA, 1979). Nevertheless, the disequilibrium nature of the natural glass shown in Fig. 5 is in accord with the experimental results.

4.2. Radial pyroxene

The present experimental results suggest that radial olivine was first formed at

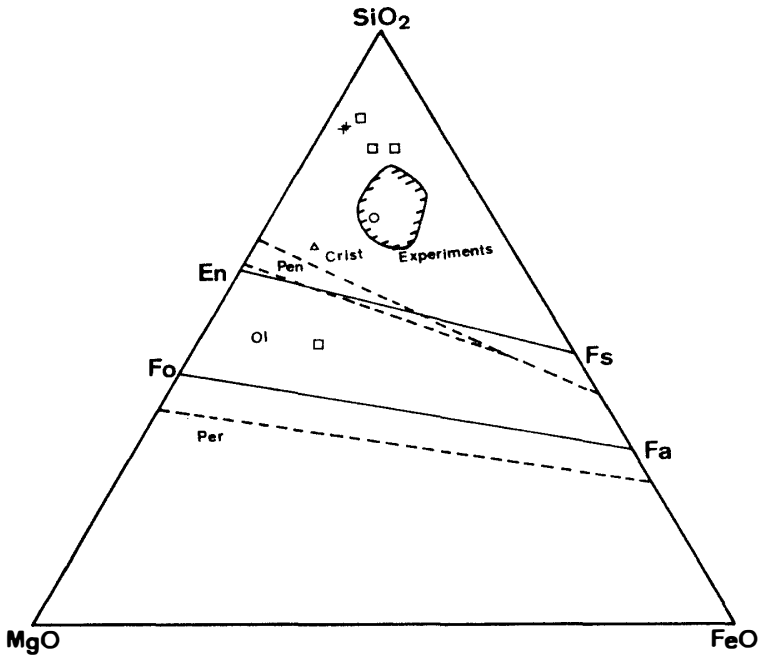

Fig. 5. Chemical compositions of the residual glasses in L3, H4 and H5 chondrites same as those in Fig. 4 except for Al_2O_3-rich ones, plotted onto the SiO_2-MgO-FeO system based on MUAN *and* OSBORN *(1965). Symbols are the same as those in Fig. 4. A hatched area shows a compositional range of the residual glass in the experiments shown in Fig. 2.*

a relatively high temperature with cooling rates of about 100 deg/min and then pyroxene was formed by reaction between radial olivine and residual SiO_2-rich liquid without changing their texture. The reaction probably took place at relatively low temperatures for a longer duration than that of crystallization. In fact, some radial chondrules were found to consist of olivine and rarely of pyroxene with patches of olivine (IKEDA and TAKEDA, 1979). Many of the chondrules with radial pyroxene texture have normative olivine (Table 5), suggesting that a first crystallizing phase is also olivine.

Actually, two cooling histories are possible to produce radial pyroxene by the mechanism proposed here, which are shown schematically in Fig. 6. During the reaction, it is not neccessary to require a geologically long duration to form radial pyroxene because the extremely SiO_2-rich residual liquid (Table 3 and Fig. 2) easily reacts with olivine. In fact, RUN 104 shows that pyroxene begins to form in about 1.5 days at 1100°C.

At present, however, there is no critical evidence for the above mechanism on the formation of radial pyroxene. Another mechanism, such as primary formation of radial pyroxene by accidental heterogeneous nucleation with external pyroxene particles, is also possible.

Table 5. Bulk chemical compositions and CIPW norms of chondrules with radial texture and of Sample No. 3.

	H5-1	L3-1	H5-2	Sample No. 3.	L3-2	L3-3		H5-1	L3-1	H5-2	Sample No. 3.	L3-2	L3-3
SiO_2	52.18	53.53	53.82	55.21	55.90	56.80	Q	-	-	-	-	-	1.51
TiO	0.30	0.10	0.18	0.00	0.14	-	Or	0.83	0.12	0.77	0.45	0.18	0.00
Al_2O_3	4.95	2.53	3.21	4.71	3.26	3.28	Ab	14.21	10.41	11.17	19.45	14.64	14.30
FeO	10.94	14.04	11.15	11.79	7.99	8.00	An	5.55	1.32	2.45	2.31	1.04	1.36
MnO	0.39	0.64	0.37	0.15	0.55	0.33	Wo	0.13	3.22	8.53	0.24	4.45	4.67
MgO	27.29	25.36	25.21	22.21	25.52	23.81	En	0.09	2.10	5.88	0.16	3.25	3.37
CaO	1.18	1.82	4.61	0.60	2.36	2.53	Fs	0.03	0.89	1.95	0.07	0.79	0.87
Na_2O	1.68	1.23	1.32	2.53	1.73	1.69	En	39.24	46.05	38.50	48.62	54.37	55.92
K_2O	0.14	0.02	0.13	0.08	0.03	-	Fs	11.73	19.54	12.80	19.06	13.23	14.43
P_2O_5		-	-	0.01	-	-	Fo	20.06	10.52	12.89	4.56	4.16	-
Total	99.05	99.27	100.00	97.37	97.48	96.44	Fa	6.61	4.92	4.72	1.98	1.12	-
							Il	0.57	0.19	0.34	0.00	0.27	0.00
							Total	99.06	99.28	100.00	97.33	97.49	96.44

H5: Yamato-74115 (NAGAHARA unpublished).
L3: Yamato-74191 (IKEDA and TAKEDA, 1979).

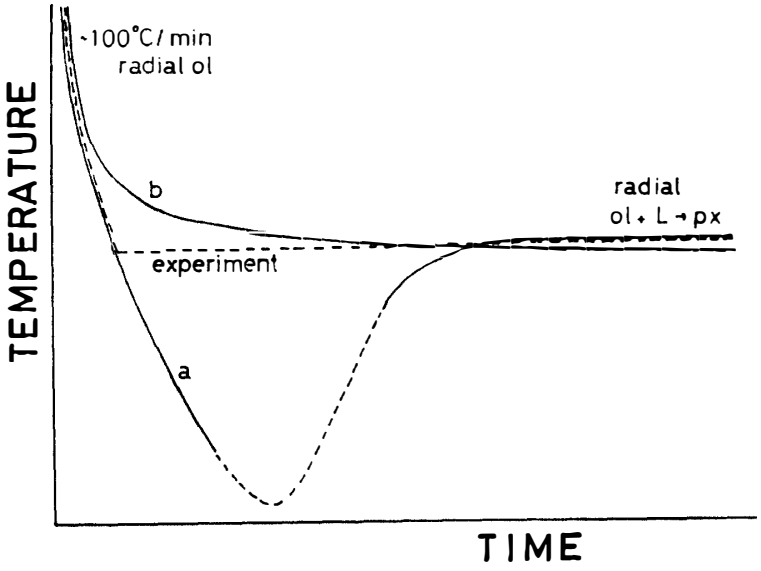

Fig. 6. Two possible cooling histories to produce radial pyroxene chondrules. The reaction between olivine and residual liquid took place by reheating process (curve a) or by significant decrease of cooling rate (curve b). Dashed line shows the cooling condition of RUN 104.

Acknowledgments

We are grateful to Prof. K. AOKI of Tohoku University for permitting the use

of X560S electron-probe microanalyzer and to Dr. H. FUJIMAKI of Tohoku University for his help in the quantitative analyses by the electron-probe microanalyzer.

References

IKEDA, Y. and TAKEDA, H. (1979): Petrology of the Yamato-74191 chondrite. Mem. Natl Inst. Polar Res., Spec. Issue, **12**, 38–58.

KIMURA, M., YAGI, K. and ONUMA, K. (1979): Classification and petrology of some Yamato chondritic meteorites. Mem. Natl Inst. Polar Res., Spec. Issue, **15**, 41–53.

KIMURA, M. and YAGI, K. (1980): Crystallization of chondrules in ordinary chondrites. Geochim. Cosmochim. Acta, **44**, 589–602.

MUAN, A. and OSBORN, E. F. (1965): Phase equilibria among oxides in steelmaking. Massachusetts, Addision-Wesley, 236 p.

ROEDER, P. L. and EMSLIE, R. F. (1970): Olivine-liquid equilibrium. Contrib. Mineral. Petrol., **29**, 275–289.

TSUCHIYAMA, A., NAGAHARA, H. and KUSHIRO, I. (1980): Experimental reproduction of textures of chondrules. Earth Planet. Sci. Lett., **48**, 155–165.

VAN SCHMUS, W. R. (1967): Polymict structure of the Mezö-Madaras chondrite. Geochim. Cosmochim. Acta, **31**, 2027–2042.

(*Received May 2, 1980*)